

Supplementary Information for

Structural insights into p300 regulation and acetylation-dependent genome organisation

Ziad Ibrahim¹, Tao Wang², Olivier Destaing², Nicola Salvi³, Naghmeh Hoghoughi², Clovis Chabert², Alexandra Rusu¹, Jinjun Gao⁴, Leonardo Feletto¹, Nicolas Reynoird², Thomas Schalch¹, Yingming Zhao⁴, Martin Blackledge³, Saadi Khochbin² & Daniel Panne^{1,*}

¹Leicester Institute of Structural and Chemical Biology, Department of Molecular and Cell Biology, University of Leicester, Leicester, UK

²CNRS UMR 5309, INSERM U1209, Université Grenoble Alpes, Institute for Advanced Biosciences, Grenoble, France.

³Institut de Biologie Structurale, CNRS, CEA, UGA, Grenoble, France

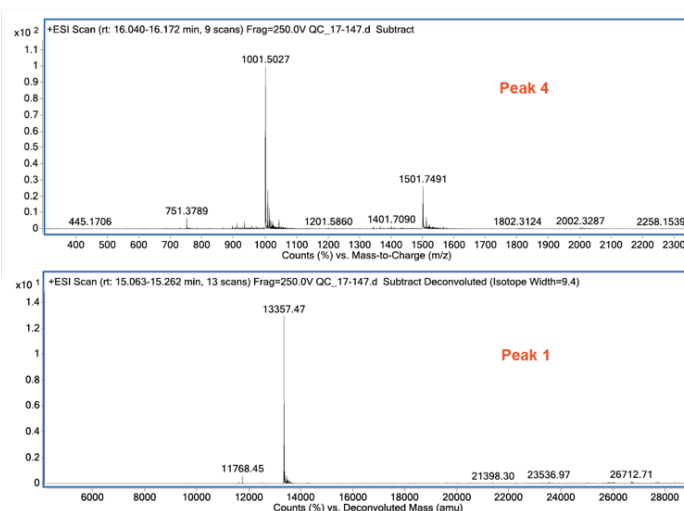
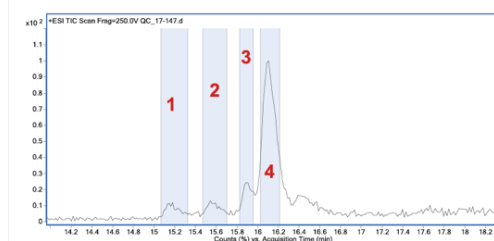
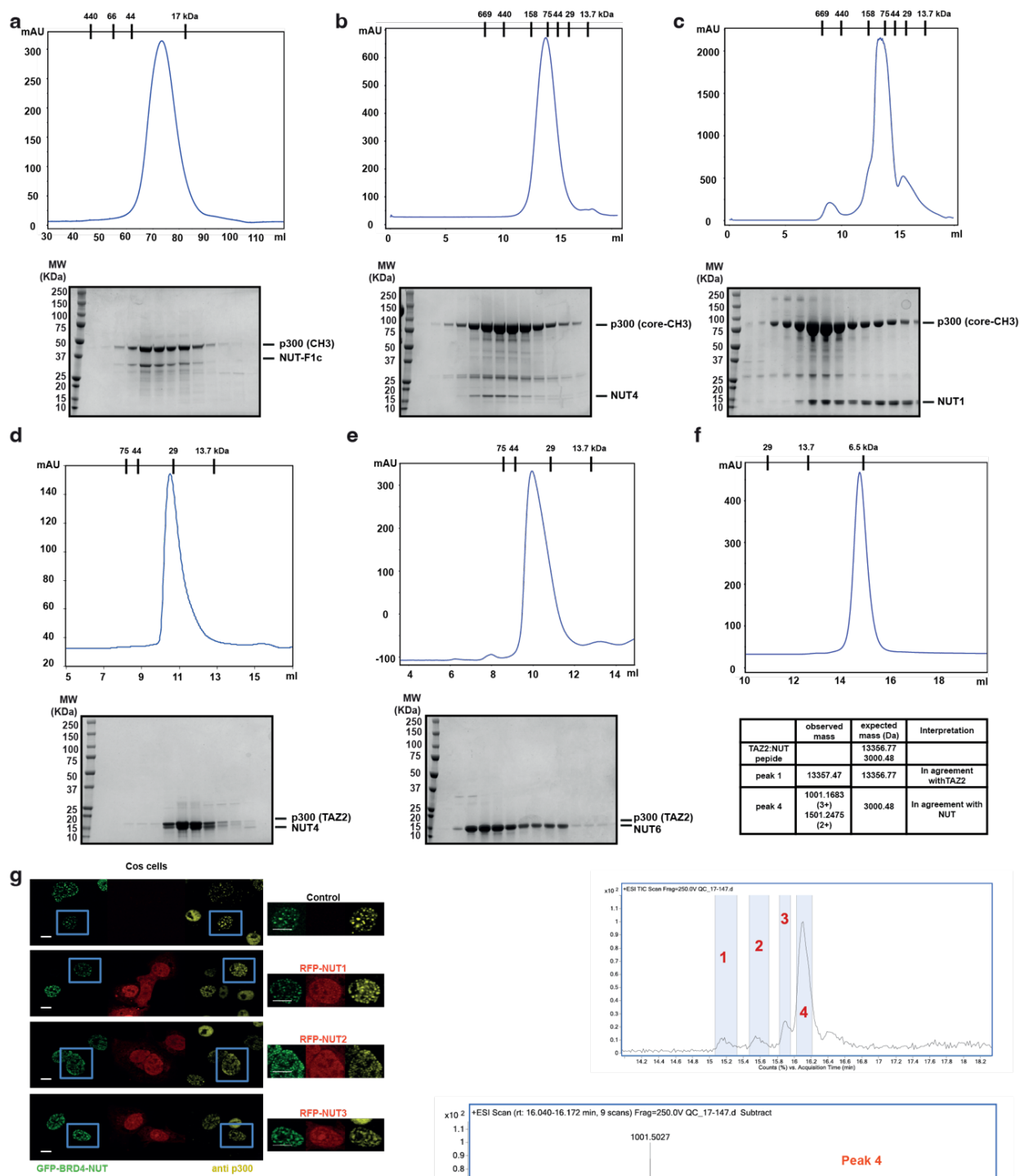
⁴Ben May Department of Cancer Research, The University of Chicago, Chicago, IL 60637, USA.

*Correspondence: daniel.panne@leicester.ac.uk

This PDF file includes:

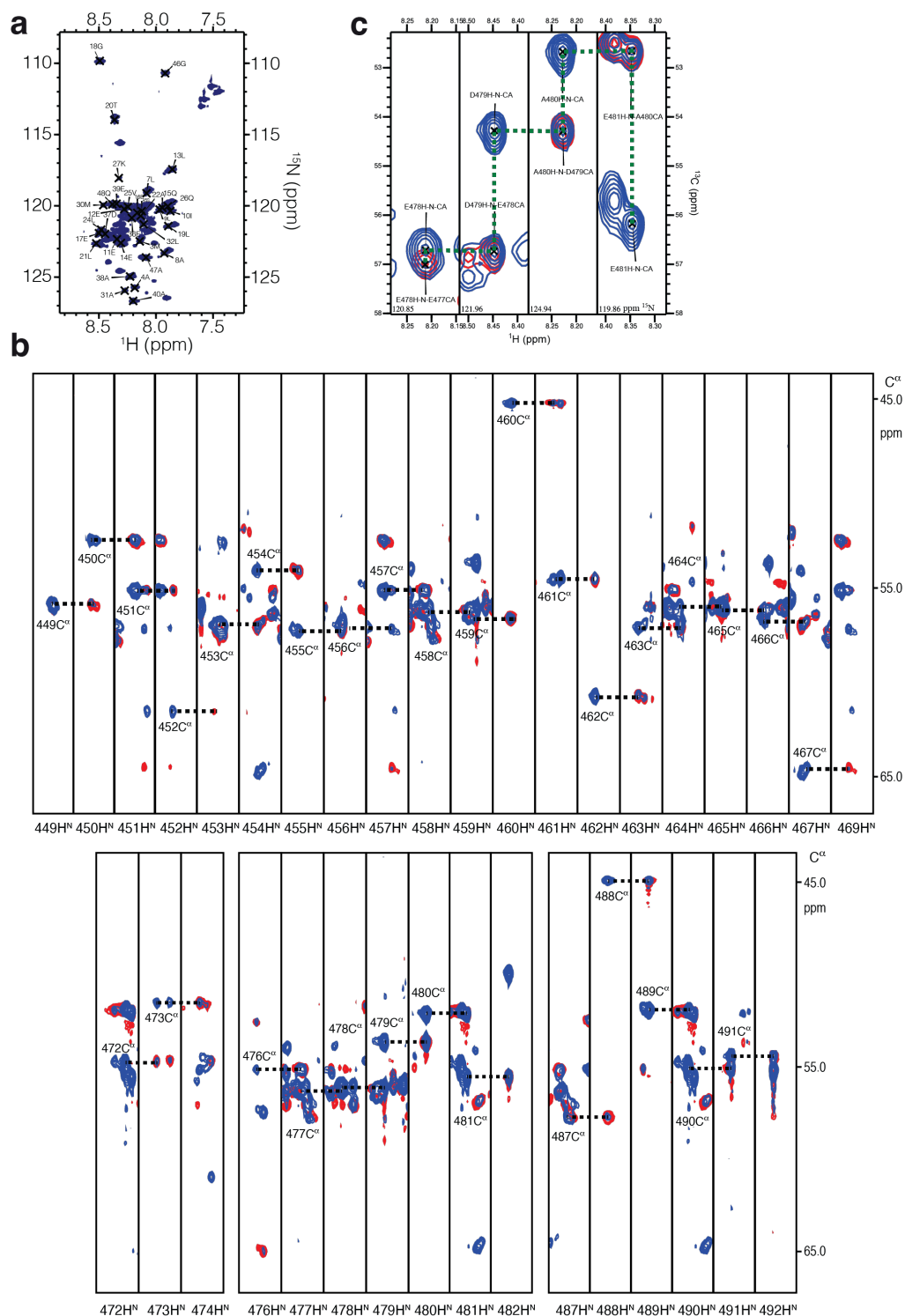
Supplementary Figures 1 to 7
Supplementary Tables 1 to 9

Legends for Supplementary Movies 1 and 2

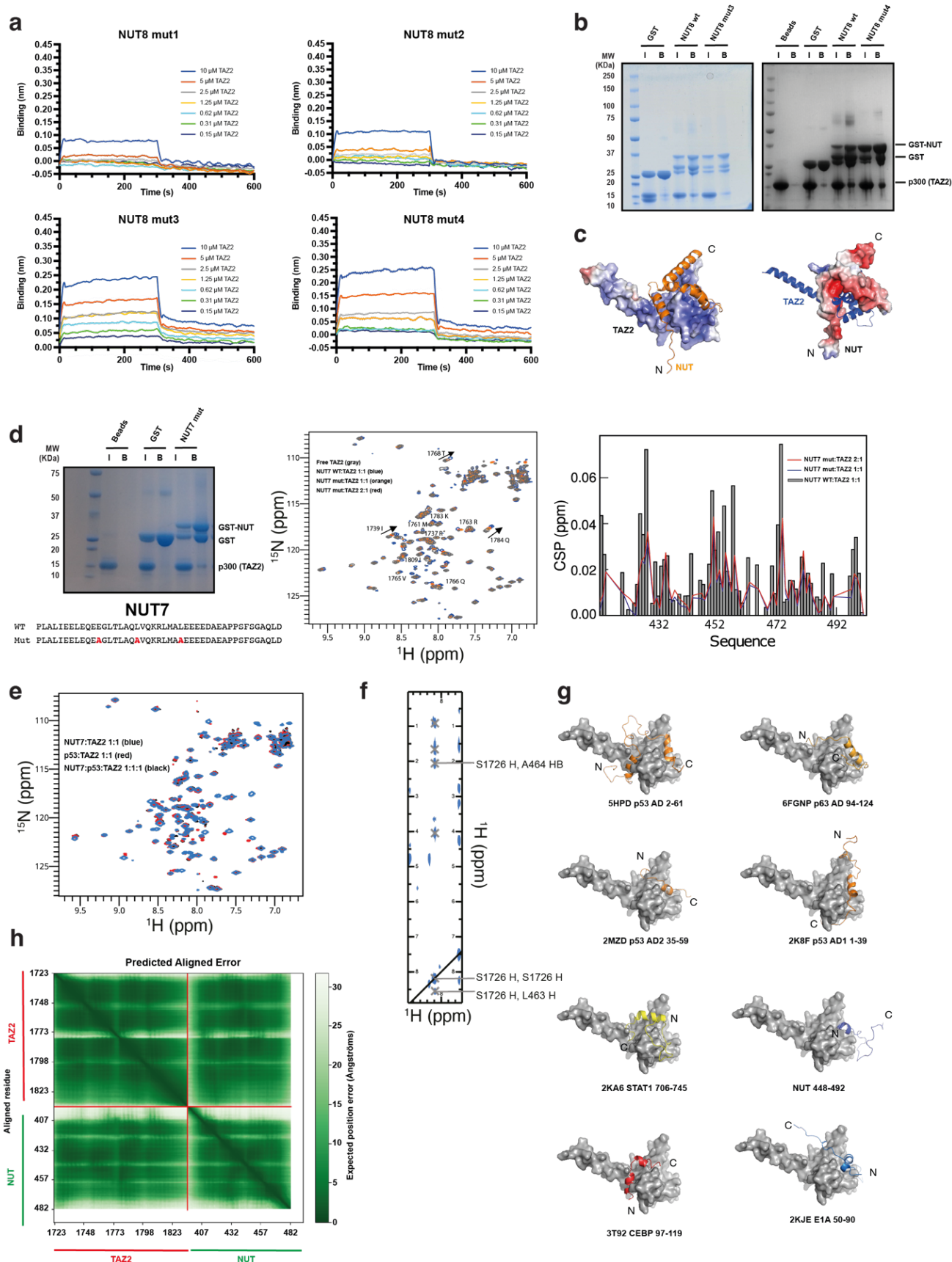


Supplementary Fig. 2. Identification of an acidic activation domain in NUT.

a, Size-exclusion chromatography (SEC) analysis of p300 CH3-NUT-F1c complex on HiLoad Superdex 200 column. **b**, SEC analysis of p300 core-CH3-NUT4 complex on Superdex 200 Increase 10/300. **c**, p300 core-CH3-NUT1 complex on Superdex 200 increase 10/300 GL. **d**, p300 TAZ2-NUT4 complex on Superdex 75 increase 10/300 GL. **e**, p300 TAZ2-NUT6 complex on Superdex 75 increase 10/300 GL. Bottom of each panel: SDS-PAGE analysis of the peak fractions. Experiments in a-e were repeated independently three times with consistency. **f**, SEC analysis of the TAZ2-NUT10 complex on Superdex 75 increase 10/300 GL column (top). Bottom: Reverse-Phase HPLC analysis of TAZ2-NUT10 peptide complex fractions followed by electrospray ionisation time of flight mass spectrometry (LC-ESI-TOF-MS). Table: Summary of the mass spectrometry analysis data showing the presence of TAZ2 (peak 1) and the NUT peptide (peak 4). **g**, Competition analysis: Cos7 cells were transfected with constructs expressing GFP-BRD4-NUT (green) alone or co-transfected with RFP-NUT1, 2 or 3 (red). Immunofluorescence with anti-p300 antibody was used to visualize condensation of endogenous p300. Experiments were repeated independently two times with consistency. Scale bars, 10 μ m.



Supplementary Fig. 3. Analysis of the TAZ2-NUT interaction. **a**, Annotated ^1H , ^{15}N HSQC spectra of NUT. **b**, Backbone assignment experiments showing magnetization transfer in HNCA (blue) and HN(CO)CA (red) experiments for the regions of NUT7(448-492) that could be assigned (experimental parameters described in Methods section). Dashed lines demonstrate correlations between neighbouring amino acids. **c**, Zoom of the same for NUT amino acids 478-481.



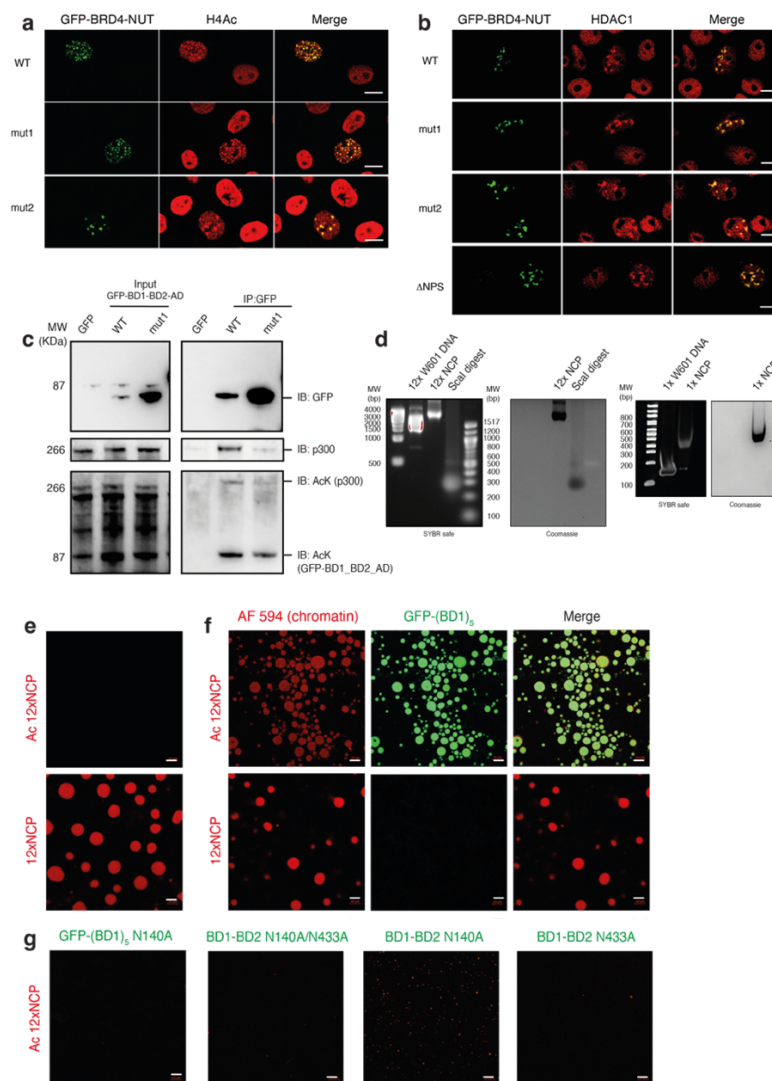
Supplementary Fig. 4. Analysis of the TAZ2-NUT interaction.

a, Representative Biolayer Interferometry (BLI) profiles of p300 TAZ2 interaction with NUT8 (396-470) mutants 1, 2, 3 and 4 from which the steady-state data shown in Fig. 3b were derived. The GST-

[illegible]

7

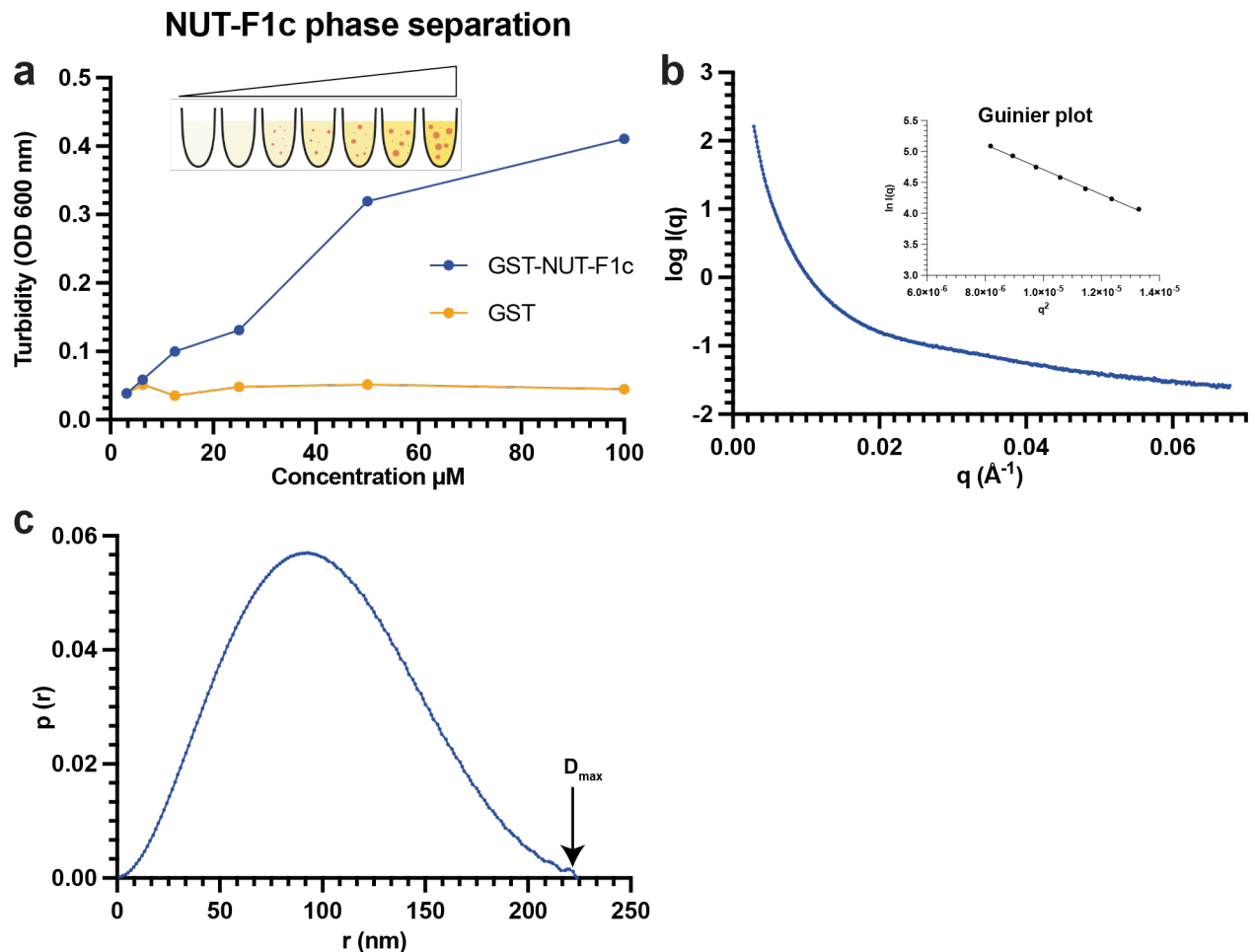
domain. **d**, NCP binding of p300 core. **e**, NCP binding of p300 core-CH3. Native PAGE gels were stained with SybrSafe DNA stain or Coomassie Blue. Experiments a-d were repeated independently at least three times. Representative data are shown. **f**, CryoEM density for the NCP used in biochemical studies. An atomic model of the NCP (PDBs: [3LZ0](#)) is docked into the density. **g**, SDS-PAGE gel showing input material used for quantitative mass spectrometry experiments. **h**, Quantitative mass spectrometry of NCP acetylation. Reconstituted NCPs were incubated with Acetyl-CoA and p300s or the p300 core. Quantification of the site-specific histone H2B, H3 and H4 acetylation by label-free HPLC/MS/MS. Data are presented as mean values \pm SD derived from n=2 independent technical replicate experiments. Source data are provided in Supplementary Data 2. **i**, Cross-link (XL-MS) analysis of the p300 core-CH3:NCP complex. p300 residues that cross-link to the NCP histones are shown in red on p300 core ([4BHW](#)) and TAZ2 ([3IO2](#)) structures. Source data are provided in Supplementary Data 1. **j**, Graphical representation of the p300:histone and histones intermolecular cross-links and intra- p300 core-CH3 cross-links. The experiment was performed once. **k**, p300 (top) and CBP (bottom) gain-of-function mutations in the TAZ2 domain.



Supplementary Fig. 6. Mechanism of condensation of BRD4-NUT and p300.

a, Colocalization of BRD4-NUT condensates with acetylated H4 (H4Ac) or **(b)** with HDAC1. Cos7 cells were transfected with the indicated GFP-BRD4-NUT constructs and analysed by immunofluorescence using anti-H4Ac antibody and anti-HDAC1 antibody. Scale bars, 10 μ m. **c**, Cos7 cells were co-transfected with HA-p300 and the indicated GFP-BRD4-NUT variants or GFP alone as the control. Co-immunoprecipitation (IP) experiments were performed using anti-GFP antibody and immuno-blotted (IB) for GFP, p300 and Acetylated-Lysine. (Left panel) Input samples were loaded as

a control. Experiments in a-c were independently repeated at least three times with consistency. **d**, EMSA analysis of 12x nucleosome templates assembly (left) on 1% agarose (12xNCP) native gels. The 12x nucleosome template was digested with *ScaI* restriction enzyme to isolate single NCPs. (Right) EMSA analysis of mononucleosome (1x NCP) assembly on 5% native PAGE stained with Sybr safe or Coomassie Blue. The experiment was repeated two times with consistency. **e**, Fluorescence microscopy images of AF594-labeled dodecameric nucleosome arrays. Non-acetylated 12x NCP chromatin formed droplets (red, bottom panel) that are dissolved after p300 acetylation (top panel). Scale bars, 10 μm . **f**, Acetylated and non-acetylated chromatin templates (red) in presence of GFP-labelled BRD4 (BD1)₅ (green). Scale bars, 10 μm . **g**, Acetylated 12x NCP chromatin with GFP-labelled BRD4 mutants. Scale bars, 10 μm . Experiment in e-g were repeated at least three times with consistency.



Supplementary Fig. 7. Condensation is driven by bromodomain multivalency.

a, Concentration-dependent droplet formation of GST-NUT-F1c (blue) in droplet formation buffer with 125 mM NaCl and 10% PEG-8000 measured by turbidity. **b**, Experimental SAXS profile (log intensities calculated as a function of momentum transfer) for a 100mM solution of GST-NUT-F1c in droplet formation buffer (blue). The Guinier region is inset. **c**, Distance distribution function. The experiment was repeated twice with consistency.

Supplementary Table 1 – List of NUT constructs and binding experiments

Sample	Amino acid residues	Binding*
NUT F1c	347-588	+
NUT1	347-446	+/-
NUT2	427-527	+
NUT3	508-588	–
NUT4	347-480	+
NUT5	347-514	+
NUT6	351-470	+
NUT7	448-492	+
NUT7 mut1	448-492	+
NUT8	396-470	+
NUT8 mut1	396-470	–
NUT8 mut2	396-470	–
NUT8 mut3	396-470	+
NUT8 mut4	396-470	+
NUT9	395-482	+
NUT10	468-482	+

*GST-pulldown, co-sedimentation or BLI

NUT7 wt: PLALIEELEQEGLTLAQLVQKRLMALEEEEDAEAPPSFSGAQLD
NUT7 mut1: PLALIEELEQEAGLTTLAQAQVQKRLMAAEEEDAEAPPSFSGAQLD
NUT8 wt: GQQQEEEGMYPDGGLLSYINELCSQKVFVSKVEAVIHPQFLADLLSPEKQRDPLALIEELEQEGLTLAQLVQKRLMALEEEEDAE
NUT8 Mut1: GQQQEEEGMYPDGGAASAINEAASQKVAASKAEAAHPQAAADAAASPEKQRAPAGAIAAAAQAAGAAQLVQKRLMALEEEEDAE
NUT8 Mut2: GQQQEEEGMYPKPGALSKINELGSQKVAGSKVSAGIHGQSLADGSSPEKQRKPLGSLIEKSEQKSGGSLAQLVQKRLMALEEEEDAE
NUT8 Mut3: GQQQEEEGMYPDGGLLSYINELCSQKVFVSKVEAVIHPQFLADLLSPEKQRAPAGAIAAAAQAAGAAQLVQKRLMALEEEEDAE
NUT8 Mut4: GQQQEEEGMYPDGGLLSYINELCSQKVFVSKVEAVIHPQFLADAAASPEKQRAPAGAIAAAAQAAGAAQLVQKRLMALEEEEDAE

Supplementary Table 2 – Chemical shifts shown in figure 2a induced by adding 1 molar equivalent of TAZ2 to ¹⁵N labelled NUT7(448-492)

Sequence	¹ H (ppm)	¹⁵ N (ppm)
449Leu	8.06773	118.78799
450Ala	7.89105	123.06117
451Leu	7.94511	120.13024
455Leu	7.84131	117.27243
457Gln	7.93157	120.03990
458Glu	8.16162	120.37610
459Glu	8.46125	121.39694
460Gly	8.44341	109.65104
461Leu	7.83935	121.27930
462Thr	8.33380	113.62034
463Leu	8.58382	122.64937
465Gln	8.30271	121.70734
466Leu	8.44144	121.21074
472Met	8.46928	119.95793
473Ala	8.30164	125.96641
474Leu	8.07340	121.83051
477Glu	8.17684	120.39170
478Glu	8.19945	120.76303
479Asp	8.43618	121.91631
480Ala	8.21909	124.95127
481Glu	8.33580	119.83160
482Ala	8.19007	126.64685
488Gly	7.92783	110.73711

489Ala	8.08558	123.65890
490Gln	8.37611	119.90610
491Leu	8.31554	124.54835
492Asp	7.90591	126.48987

Supplementary Table 3 - HADDOCK docking statistics

Distance constraints	
Ambiguous interaction restraints (AIRs)	14
Active residues on NUT7	5
Active residues on TAZ2	9
Intermolecular NOEs	2
Dihedral angle restraints*	
Phi/Psi	5/5
Structural statistics	
AIR Violations (mean \pm s.d.)	2 ± 1
Ramachandran analysis	
Residues in the favoured region (%)	87%
Residues in the additional allowed regions (%)	10%
Outliers	3%
Intermolecular energies after water refinement	
E_{vdw} (kcal mol ⁻¹)	-45 ± 7
E_{elec} (kcal mol ⁻¹)	-303 ± 32
Buried surface area (Å ²)	1498 ± 88

*Dihedral angle restraints derived from chemical shift values using TALOS-N are applied to NUT7 only. For the TAZ2 domain, the structure in PDB 2mzd is used as input to HADDOCK.

Supplementary Table 4 - Cryo-EM data collection and map reconstruction

Nucleosome Core Particle	
Data collection	FEI Titan Krios G3
Detector	Gatan K3 direct electron detector
Voltage	300 kV
Pixel size (Å)	1.086
Nominal Magnification	81,000
Dose rate on Detector (e ⁻ sec ⁻¹ px ⁻¹)	15
Dose rate on specimen (e ⁻ sec ⁻¹ px ⁻¹)	17
Defocus range (μm)	-2.3 to -1.1
Reconstruction	
Symmetry imposed	C1
Initial particle images (no.)	80,764
Final particle images (no.)	33,202
Resolution, FSC=0.143 (Å)	6.61

Supplementary Table 5 – Quantification of condensation of BRD4-NUT variants*

GFP-BRD4-NUT	RFP-p300 positive	RFP-p300 negative
WT	100/100	100/100
mut1	99/100	89/100
mut2	100/100	92/100
BD1-BD2	16/100	0/100
BD1	18/100	0/100
BD2	99/100	99/100
K/E	21/100	3/100
ΔNPS	100/100	100/100
ΔBID	100/100	9/100
BD1-BD2-AD	99/100	1/100
BD1-BD2-ADmut1	0/100	0/100
BD1-BD2-E1A	94/100	91/100

* Foci forming cells/Total cell count

Supplementary Table 6 – Quantification of co-localization of BRD4-NUT and p300*

GFP-BRD4-NUT	Pearson's R value	Co-localization ratio
WT	0.81±0.01	0.90±0.02
ADmut1	0.84±0.01	0.87±0.02
ADmut2	0.76±0.02	0.90±0.01
ΔNPS	0.76±0.02	0.86±0.03

* At least 10 cells were analysed (n=10)

Supplementary Table 7 – Impact of Drug treatment on condensation

GFP-BRD4-NUT	JQ1	A485	TSA	CBP30	1,6-Hexandiol
WT	No	No	No	Yes	No
ADmut1	No	No	No	No	No
ADmut2	No	No	No	No	No
ΔNPS	No	No	No	Yes	No

Supplementary Table 8 – Quantification of foci formation of after CBP30 treatment*

GFP-BRD4-NUT	DMSO	CBP30
WT	100/100	54/100
ADmut1	92/100	3/100
ADmut2	91/100	2/100
ΔNPS	100/100	58/100

*Foci-forming cells/Total cell counted

Supplementary Table 9 – SAXS data analysis

Sample	GST-NUT-F1c
Guinier Analysis	Sample (GST-NUT-F1c)
$I(0)$ (cm ⁻¹)	0.8159E+03
R_g (Å)	771.84
q -range (Å ⁻¹)	0.00286 to 0.00365
$P(r)$ analysis	Sample (GST-NUT-F1c)
$I(0)$ (cm ⁻¹)	0.8159E+03
R_g (Å)	773.00
d_{max} (Å)	2283
q -range (Å ⁻¹)	0.0029 to 0.0678